

Extension of Geometric Scaling to Large x

Miguel N. Mondragon ^a, J.G. Contreras ^{a,*}

^a *Departamento de Física Aplicada, Centro de Investigación y Estudios Avanzados del I.P.N., Unidad Mérida, Apartado Postal 73 Cordemex, Mérida Yucatán 97310, México.*

Abstract

We perform a detailed analysis on the validity of geometric scaling in the total γ^*p cross section, σ_{γ^*p} . We propose to separate the small and large x behavior writing σ_{γ^*p} as a product of two functions W and S representing, respectively, the dynamical degrees of freedom dominant at small x and a contribution only important at large x . Defining a reduced cross section $\tilde{\sigma}_{\gamma^*p} \equiv \sigma_{\gamma^*p}/S$, we observe geometric scaling for $\tilde{\sigma}_{\gamma^*p}$ over nine orders of magnitude, up to the highest measured values of x and Q^2 .

Key words: Geometric Scaling, Deeply Inelastic Scattering

PACS: 13.60.Hb

1 Introduction

It has been found that for low values of the Bjorken variable x , $x \leq 0.01$, the total γ^*p cross section, $\sigma_{\gamma^*p}(x, Q^2)$, extracted from lepton–hadron scattering presents the property of geometric scaling [1,2]. This property permits to write the cross section as a function of only one variable, τ , called the scaling variable, which is the product of two functions, one depending only on Q^2 and the other only on x . It has been suggested that, for σ_{γ^*p} , τ is given by Q^2/Q_s^2 with $Q_s^2 = Q_s^2(x)$ known as the saturation scale. Geometric scaling has also been observed in eA reactions [3], inclusive charm production [4] and nucleus–nucleus collisions [5].

The observation that σ_{γ^*p} grows quite rapidly at low x and that this behavior cannot continue indefinitely without violating the unitarity of the cross

* Corresponding author.

Email address: jgcn@mda.cinvestav.mx (J.G. Contreras).

section led to the proposal of nonlinear QCD equations containing saturation [6,7,8,9,10,11]. One of the features of this type of equations is the introduction of a scale, Q_s^2 , to signal the onset of saturation effects. Much of the excitement and advance in the understanding of perturbative QCD at low x in recent years comes from the discovery that some saturation equations imply geometric scaling at the saturation scale [12,13,14,15].

Much recent theoretical work has been devoted to find both, the region where geometric scaling is valid and the functional form of the violations to geometric scaling above the saturation scale. Studies based on the BFKL equation [16] supplemented with specific boundary conditions have found that there is a window of phase space above Q_s^2 and below a Q_{\max}^2 on which geometric scaling is valid. For current accessible energies, Q_{\max}^2 is of the order of 100 GeV² [17,18,19]. More recently, there have been indications that, in a more general nonlinear equation, geometric scaling is strongly violated [20]. None of these investigations expect geometric scaling to be valid far away from Q_s^2 .

In this Letter we show how to extend geometric scaling to all values of x and Q^2 . We perform a detailed analysis on the departure of the total γ^*p cross section from the geometric scaling behavior as the virtuality of the process grows with respect to the saturation scale leading to the region where $Q^2 \gg Q_s^2$. We propose to write the total γ^*p cross section as

$$\sigma_{\gamma^*p} = W(x, Q^2)S(x), \quad (1)$$

where $W(x, Q^2)$ has all the information on the dynamical degrees of freedom at small x and $S(x)$ is a Q^2 -independent distribution which mainly contributes to the large x region. This separation of small and large x behavior is reminiscent of the general ideas which form the basis of the Color Glass Condensate (CGC) [9]. We show that the reduced cross section $\tilde{\sigma}_{\gamma^*p} \equiv W(x, Q^2)$ displays geometric scaling in the complete kinematic plane. We use $\tilde{\sigma}_{\gamma^*p}$ to find *i*) that geometric scaling is exact below $Q^2 \approx 1$ GeV² and *ii*) a functional form describing geometric scaling violations which turn out to depend on the logarithm of Q^2 . Our results also yield a natural six parameter description of all data on σ_{γ^*p} for $Q^2 > 1$ GeV².

2 Geometric Scaling Behavior of $\tilde{\sigma}_{\gamma^*p}$

First we turn to the behavior of σ_{γ^*p} at small x from the point of view of geometric scaling. There are several definitions of the saturation scale $Q_s^2(x)$ used to define the scaling variable τ . We work with the one used by K. Golec-Biernat and M. Wüsthoff [21]. They proposed that $Q_s^2(x) \sim x^{-\lambda_s}$ with $\lambda_s =$

0.288. On the other hand St  sto *et al.* [1] found that, for $\tau = Q^2/Q_s^2(x) > 1$, $\sigma_{\gamma^*p}(\tau) \sim 1/\tau$ suggesting a power law behavior of σ_{γ^*p} as a function of x for constant values of Q^2 . From the point of view of theory, BFKL evolution also predicts a power law behavior at small x for σ_{γ^*p} . Following these results we propose to write $W(x, Q^2)$ in equation (1) as

$$W(\bar{x}, Q^2) = N\bar{x}^{-\lambda}, \quad (2)$$

where following [21], we use \bar{x} instead of x –Bjorken. Both are related through

$$\bar{x} = x \left(1 + \frac{4m_f^2}{Q^2} \right), \quad (3)$$

with $m_f = 140$ MeV. Note that x and \bar{x} are substantially different only at very low Q^2 .

In equation (2) $N = N(Q^2)$ gives the normalization. The exponent λ may be different for different Q^2 values as found at HERA [22]. $W(x, Q^2)$ represents then the small x behavior of the total cross section σ_{γ^*p} .

Turning now to the large x region, we require from S to be approximately constant at small x , so that it does not alter the physics embodied in W , and that it describes the cross section at large x . We found that a Gaussian distribution is an adequate choice for S :

$$S(\bar{x}) = \frac{1}{\sqrt{2\pi\sigma^2}} \exp\left(-\frac{(\bar{x} - x_0)^2}{2\sigma^2}\right). \quad (4)$$

We use data from fix target [23,24] and HERA [25,26] experiments to compare against equation (1). We fit the data for each fixed Q^2 value. As an example, Figure 1 shows data from HERA and fixed target experiments at $Q^2=15$ GeV 2 .

Figure 1 is very well described by the proposed functional form from equation (1). Furthermore, the same can be said at each value of Q^2 where there are measured points from both, fixed target and HERA experiments. Interestingly we find that x_0 and σ^2 from equation (4) do not depend on Q^2 . They take the values $x_0 = 0.27$ and $\sigma^2 = 0.07$.

It follows then, that it is indeed possible to separate the small and large x behavior of the cross section and that this separation can be phrased in the language of the CGC [9]. At large x we find a Gaussian distribution which do not depend on Q^2 and it is constant at small x . That is, $S(x)$ describes a static valence-like distribution of color charges. On the other hand, $W(x, Q^2)$ is a power law at each fixed value of Q^2 exactly as expected for dynamical degrees

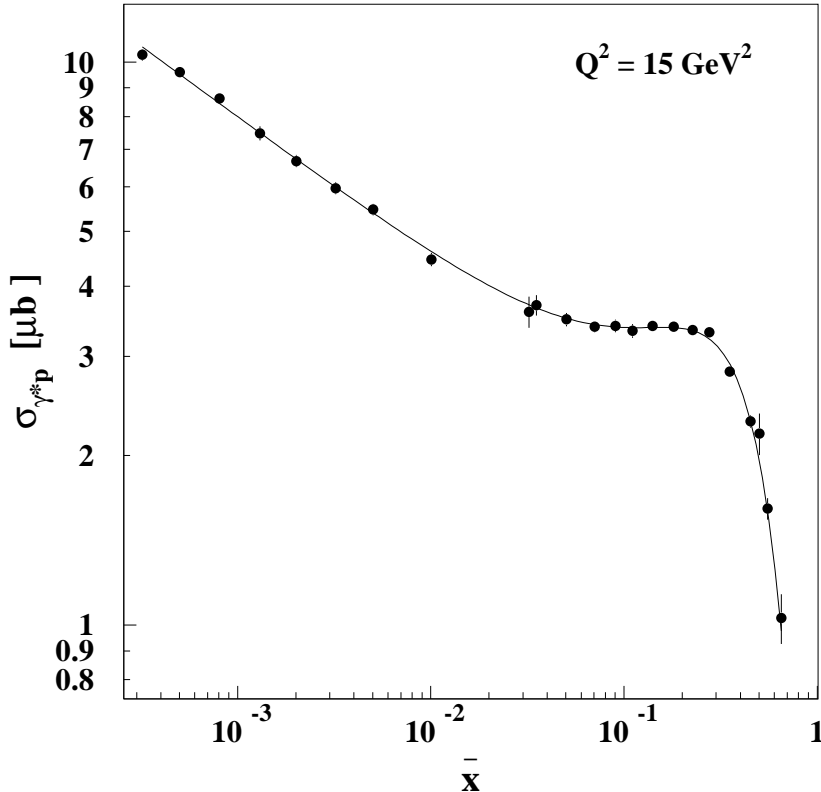


Fig. 1. The total $\gamma^* p$ cross section is shown as a function of \bar{x} for $Q^2=15$ GeV 2 . The points are experimental data from fixed target and HERA experiments and the line is a fit to the form of equations (1–4). A power law is clearly seen at low values of \bar{x} , while the structure at high \bar{x} corresponds to a Gaussian distribution.

of freedom carried by wee partons. Note that the CGC is not a model, but it has very solid foundations being a semi-classical approximation of QCD for a high density regime. From this point of view the description of equation (1) using CGC-like ideas provides a link between our phenomenological results and a theoretical QCD-based framework.

The geometric scaling discovered by Stásto *et al.* [1] is valid only for the small x region $x < 0.01$. This means that it is valid for the region where the power law dominates (see Figure 2). In our approach S can be considered constant in this region and all the dynamics is in W , thus we defined the reduced cross section $\tilde{\sigma}_{\gamma^* p}$ as

$$\tilde{\sigma}_{\gamma^* p} \equiv W(x, Q^2) = \sigma_{\gamma^* p} / S(x) \quad (5)$$

to isolate the power law behavior in the total cross section. Remarkably, we find that the reduced cross section $\tilde{\sigma}_{\gamma^* p}$ displays geometric scaling at all measured values of x and Q^2 .

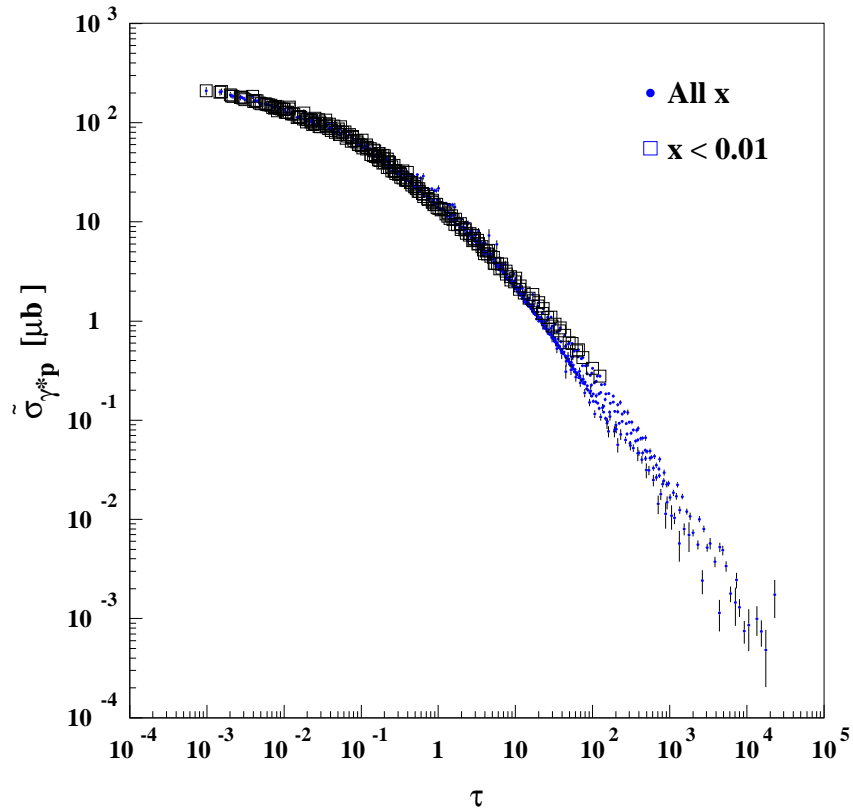


Fig. 2. The reduced $\gamma^* p$ cross section, $\tilde{\sigma}_{\gamma^* p}$, is shown as a function of the scaling variable $\tau = Q^2 x^{\lambda_s}$ with $\lambda_s = 0.288$ [21] for all data in [23,24,25,26], which span six orders of magnitude in both of each x and Q^2 . The geometric scaling behavior is clearly seen over nine orders of magnitude in τ . Data points in the small x region, $x < 0.01$ are also shown as empty squares to have a comparison with previous studies [1].

The data span six orders of magnitude both in x , from $0.62 \cdot 10^{-6}$ to 0.75 , and in Q^2 , from 0.045 to 30000 GeV^2 . This scaling behavior, extending over almost nine orders of magnitude in $\tau = Q^2 x^{\lambda_s}$ is shown in Figure 2. Note that here, and in the following when needed, it is assumed that Q^2 is divided by a constant of value 1 GeV^2 so that the scaling variable is dimensionless. This figure shows all the data, and separately the data restricted to the region $x < 0.01$ studied in previous analysis [1]. With the addition of data with $x > 0.01$ the geometric scaling behavior is extended two orders of magnitude in τ . It is quite interesting to compare Figure 2 with Figure 4. This latter figure contains all data points with $Q^2 \geq 1.5 \text{ GeV}^2$ before the data collapse produced by the transformation to the scaling variable τ .

3 Q^2 Dependence of λ and N

We use all HERA data [25,26] to fit the reduced cross section $\tilde{\sigma}_{\gamma^* p}$ to a power law for constant values of Q^2 . We do not use fixed target data at this stage of the analysis, because those data points are concentrated at high x and thus, they do not have a lever arm long enough to determine accurately the power law parameters. Their influence has already been taken into account through the definition of $S(x)$.

There are 43 different experimental Q^2 values, ranging from 0.085 to 20000 GeV^2 , with enough data points in x to perform the fit. The average number of points for each fit was 8, ranging from 3 to 12. At each value of Q^2 , equation (2) provides an excellent description of data. The results for N and λ for each individual fit are quite precise and provide a clear picture of their Q^2 dependence as shown in Figure 3.

We observe a dramatic change in the behavior of both functions, $N(Q^2)$ and $\lambda(Q^2)$ when the virtuality of the photon approaches from above the region around 1 GeV^2 . In the following we denote this threshold with Q_o^2 . Below this scale both N and λ are constants denoted by N_o and λ_o respectively. They take the following approximate values: $N_o \approx 40 \mu\text{b}$ and $\lambda_o \approx 0.1$. In particular the value of λ_o is, as expected, very similar to the one found with the Donnachie–Landshoff parametrization [27].

For all Q^2 values below Q_o^2 there is a strong form of geometric scaling. Not only λ is independent of Q^2 , but also N is, thus the total cross section, $\sigma_{\gamma^* p}$, depends only on one variable. But this form of saturation due to the smallness of Q^2 is different from the saturation due to high density effects in a region of weak coupling.

Turning now to values of Q^2 above Q_o^2 we find that $\lambda(Q^2)$ behaves as

$$\lambda(Q^2) = a + \alpha \log(Q^2), \quad (6)$$

while $N(Q^2)$ behaves as the power law

$$N(Q^2) = b Q^{2\beta}. \quad (7)$$

A fit in the intermediate Q^2 region to the data plotted in Figure 2 yields $b = 28.2 \pm 0.9 \mu\text{b}$, $\beta = -1.110 \pm 0.006$, $a = 0.101 \pm 0.006$ and $\alpha = 0.060 \pm 0.001$. The quality of the fits is $\chi^2/dof = 0.6145$ and $\chi^2/dof = 0.3598$ for $N(Q^2)$ and $\lambda(Q^2)$ respectively. Note that the points at the largest Q^2 were not taken into account, because they have big fluctuations due to the limited statistics of data.

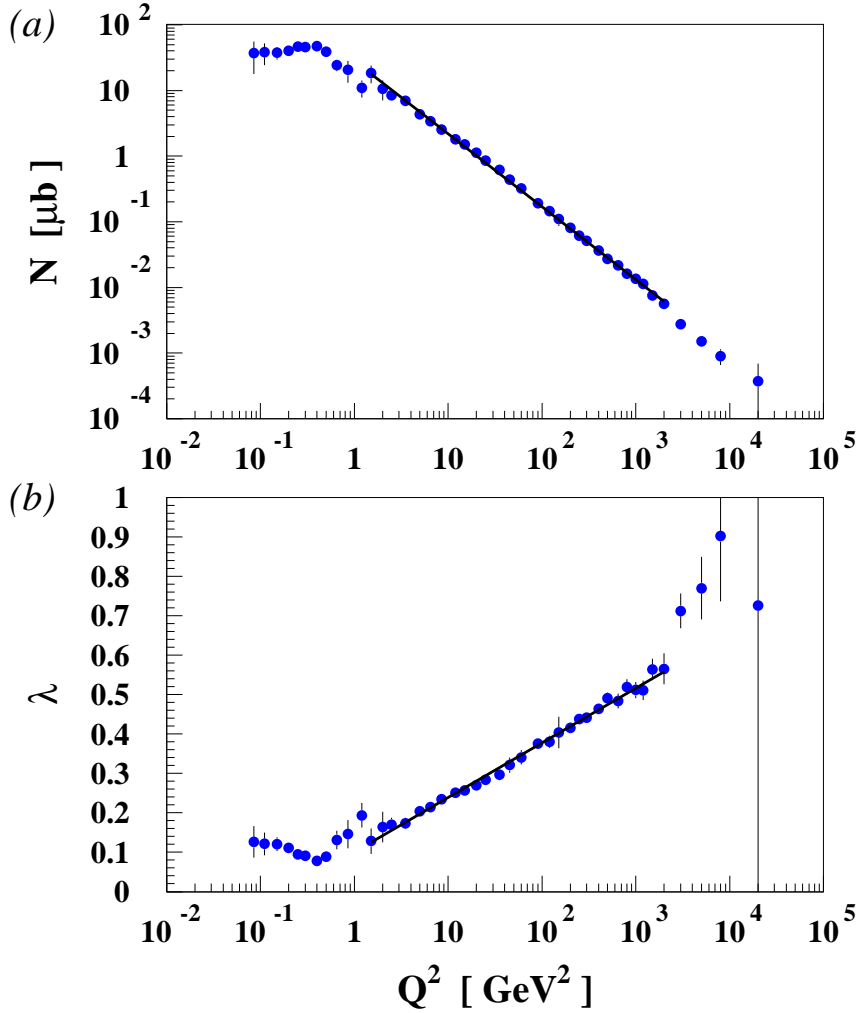


Fig. 3. The Q^2 dependence of the normalization (a) and the exponent (b) of $\tilde{\sigma}_{\gamma^* p} = N x^{-\lambda}$, extracted from fits to the reduced cross section $\tilde{\sigma}_{\gamma^* p}$ at fixed values of Q^2 . The solid lines are fits to $N(Q^2) = b Q^{(2\beta)}$ (a) and to $\lambda(Q^2) = a + \alpha \log(Q^2)$ (b) in the intermediate Q^2 range.

Above Q_o^2 there is no exact geometric scaling and its violations follow *i*) a power law in the normalization as seen in equation (7), and *ii*) the Q^2 logarithmic dependence on the exponent shown in equation (6).

Our results explain the success of geometric scaling for small x . Note that $x < 0.01$ implies $Q^2 < 450 \text{ GeV}^2$, which corresponds to $\lambda < 0.46$. So $\lambda = 0.288$ is the intermediate value between 0.46 and λ_o . Note also that the slope of N , $\beta = -1.110 \pm 0.006$, is very close to minus one. Finally, note that the Gaussian distribution $S(x)$ can be considered constant over this range. Under these conditions

$$\sigma_{\gamma^* p} \sim \frac{1}{Q^2 x^\lambda} = \frac{1}{Q^2 x^{\lambda_s}} x^{\lambda_s - \lambda} = \frac{1}{\tau} x^{\lambda_s - \lambda}. \quad (8)$$

The exponent $\lambda_s - \lambda$ is small and its influence is partially compensated by the Q^2 dependence of the normalization. The ranges in x for fixed Q^2 go from one to one and a half orders of magnitude, so that there is not enough phase space to notice the change in the slope λ . The same arguments can be applied to the reduced cross section $\tilde{\sigma}_{\gamma^* p}$ explaining why scaling also holds for it.

The important physics message behind these quantitative arguments is twofold:
 i) The exponent of Q^2 , β , in the normalization of equations (2,7) is fixed and
 ii) the slope λ varies slowly with the logarithm of Q^2 . This suggests that a function which incorporates power law behavior in both, x and Q^2 could be a good candidate to solve the nonlinear equations at Q_o^2 and below it, and could also be a good candidate to expand the solution above this scale.

Equations (7,6) contain all the dynamical information regarding the evolution in phase space from one Q^2 point to another. Note that they have a very simple form and that in principle they could be considered the solution of a DGLAP [28] type of evolution equation.

4 A simple model for the total $\gamma^* p$ cross section above Q_o^2 .

Note that as a spin off of the description of $\sigma_{\gamma^* p}$ given by equation (1) we also have a simple six parameter description of the total $\gamma^* p$ cross section for *all* Q^2 values above Q_o^2 :

$$\sigma_{\gamma^* p}(\bar{x}, Q^2) = b Q^{2\beta} \bar{x}^{-(a+\alpha \log(Q^2))} \frac{1}{\sqrt{2\pi\sigma^2}} \exp\left(-\frac{(\bar{x} - x_0)^2}{2\sigma^2}\right). \quad (9)$$

Equation (9) is compared to the data in Figure 4 using the parameters obtained from the fit to Figure 2. For these parameters the χ^2/dof obtained for $Q^2 \geq 1.5$ GeV 2 is $\chi^2/dof = 0.96$ for 622 data points. The quality of the χ^2 is similar for HERA ($\chi^2/dof = 0.86$, $n = 298$) and fixed target experimental data ($\chi^2/dof = 1.08$, $n = 324$).

5 Summary and conclusions

We have shown that $\sigma_{\gamma^* p}$ can be separated as a product of a power law carrying all the information on its Q^2 evolution and a Gaussian distribution which depends only on x . This separation can be described with CGC-like ideas. We define a reduced cross section $\tilde{\sigma}_{\gamma^* p}$ using the power law part of $\sigma_{\gamma^* p}$. We find geometric scaling behavior for $\tilde{\sigma}_{\gamma^* p}$ in the complete kinematic plane. As

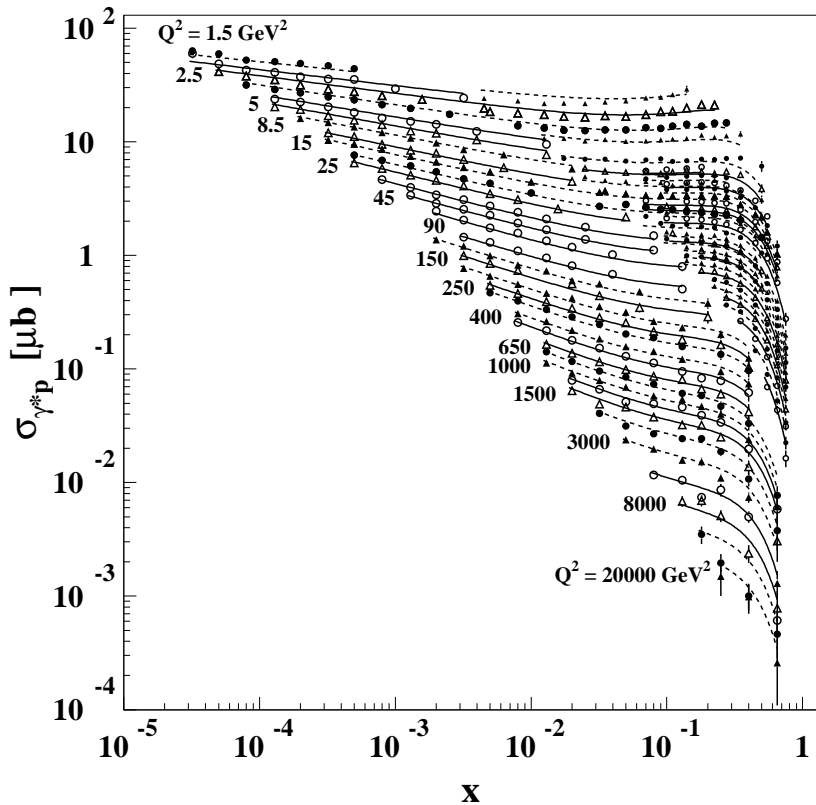


Fig. 4. The total $\gamma^* p$ cross section, $\sigma_{\gamma^* p}$, is shown as a function of x for different fixed values of Q^2 . The bullets are the experimental data points, while the lines are the result of equation (9).

a spin-off of this description, we obtain a natural parametrization of all $\sigma_{\gamma^* p}$ data above $Q^2 \approx 1 \text{ GeV}^2$.

These results could be used as a guideline to look for exact solutions to saturation equations at the saturation scale or to look for approximate solutions at higher virtualities. They also suggest that a formulation of $\sigma_{\gamma^* p}$ as a product of power laws in x and Q^2 is a suitable way to describe the energy dependence of the saturation scale.

Acknowledgments This work has been partially supported by Conacyt through grant 40073-F.

References

- [1] A.M. St  sto, K. Golec-Biernat and J. Kwieci  ski, Phys. Rev. Lett. **86**, 596 (2001).
- [2] Schildknecht, B. Surrow and M. Tentyukov, Phys. Lett. B **499**, 116 (2001).

- [3] A. Freund, K. Rummukainen, H. Weigert and A. Schäfer Phys. Rev. Lett. **90**, 222002 (2003).
- [4] V. P. Goncalves and M.V.T. Machado, Phys. Rev. Lett. **91**, 202002 (2003).
- [5] N. Armesto, C. A. Salgado and U. A. Wiedemann, Phys. Rev. Lett. **94**, 022002 (2005).
- [6] L.V. Gribov, E.M. Levin and M.G. Ryskin, Phys. Rep. **100**, 1 (1983).
- [7] E.M. Levin and M.G. Ryskin, Phys. Rep. **189**, 267 (1990).
- [8] A.H. Mueller and J. Qiu, Nucl. Phys. B **268**, 427 (1986); J. P. Blaizot and A. H. Mueller, Nucl. Phys. B **289**, 847 (1987).
- [9] L. McLerran, R. Venugopalan, Phys. Rev. D **49** 2233 (1994); **49**, 3352 (1994); **50**, 2225 (1994).
- [10] I. Balitsky, Nucl. Phys. B **463**, 99 (1996).
- [11] Yu. V. Kovchegov, Phys. Rev. D **60**, 034008 (1999).
- [12] J. Bartels and E. Levin, Nucl. Phys. B **387**, 617 (1992).
- [13] E. Levin and K. Tuchin, Nucl. Phys. B **573**, 833 (2000); Nucl. Phys. A **691**, 779 (2001); **693**, 787 (2001).
- [14] E. Iancu and L. McLerran, Phys. Lett. B **510**, 145 (2001).
- [15] S. Munier and R. Peschanski, Phys. Rev. Lett. **91**, 232001 (2003).
- [16] E.A. Kuraev, L.N. Lipatov and V.S. Fadin, Sov. Phys. JETP **45**, 199 (1977); Ya.Ya. Balitsky and L.N. Lipatov, Sov. J. Nucl. Phys. **28**, 22 (1978).
- [17] J. Kwieciński and A.M. Stasto, Phys. Rev. D **66**, 014013 (2002);
- [18] E. Iancu, K. Itakura, and L. McLerran, Nucl. Phys. A **708**, 327 (2002);
- [19] A.H. Mueller and D.N. Triantafyllopoulos, Nucl. Phys. B **640**, 331 (2002); D.N. Triantafyllopoulos, Nucl. Phys. B **648** 293 (2003).
- [20] A. H. Mueller and A. I. Shoshi, Nucl. Phys. B **692**, 175 (2004); E. Iancu, A.H. Mueller and S. Munier, Phys. Lett. B **606**, 342 (2005).
- [21] K. Golec-Biernat and M. Wüsthoff, Phys. Rev. D **59**, 014017 (1999); **60**, 114023 (1999).
- [22] H1 Collab., C. Adloff *et al.*, Phys. Lett. B **520**, 183 (2001).
- [23] BCDMS Collaboration, A.C. Benvenuti *et al.*, Phys. Lett. B **223**, 485 (1989).
- [24] NMC Collaboration, M. Arneodo *et al.*, Nucl. Phys. B **483**, 3 (1997);
- [25] H1 Collab., C. Adloff *et al.*, Eur. Phys. J. C **19**, 269 (2001); **21**, 33 (2001); **30**, 1 (2003).

- [26] ZEUS Collab, J. Breitweg *et al.*, Phys. Lett. B **487** 53 (2000).
- [27] A. Donnachie and P.V. Landshoff, Phys. Lett. B **296**, 227 (1992).
- [28] Yu. L. Dokshitzer, Sov. Phys. JETP **46**, 641 (1977); V. N. Gribov and L. N. Lipatov, Sov. J. Nucl. Phys. **15**, 438 (1972); G. Altarelli and G. Parisi, Nucl. Phys. B **126**, 298 (1977).